

Electron-impact ionization of laser-excited $^{138}\text{Ba}(\dots 5p^6 6s 6p)$ and $^{138}\text{Ba}(\dots 5p^6 6s 5d)$ atoms

S. Trajmar, J. C. Nickel,* and T. Antoni†

Jet Propulsion Laboratory, California Institute of Technology, Pasadena, California 91109

(Received 21 July 1986)

Electron-impact ionization cross sections for laser-excited $^{138}\text{Ba}(\dots 5p^6 6s 6p; ^1P_1, M = -1)$ and cascade-populated $^{138}\text{Ba}(\dots 5p^6 6s 5d; ^1D + ^3D)$ atoms were measured in the threshold to 10 eV energy range. The peak cross sections for the excited species are about a factor of 2 larger than that for ground-state Ba. In addition, it was demonstrated that ionization from individual magnetic substates of various hyperfine levels can be studied. The ionization cross sections in the case of $^{138}\text{Ba}(^1P_1)$ were found to be equal for the $M=0$ and for the $M = \pm 1$ sublevels within the experimental error limit.

Electron-impact ionization cross sections have been measured for a large number of ground-state atomic species and for some ground-state ions.¹ With the exception of a few metastable species, cross sections for excited atoms are not available. The main reason for the absence of ionization data for excited species is the experimental difficulty associated with the generation of suitable concentration (or flux) of excited atoms for such measurements. With the availability of tunable lasers one can, however, overcome this problem. We applied the laser excitation technique to Ba and measured ionization cross sections for $^{138}\text{Ba}(\dots 6s 6p; ^1P_1, M = -1)$ and $^{138}\text{Ba}(\dots 6s 5d; ^1D$ and 3D , averaged over magnetic substates) species in the threshold to 10 eV impact energy range. Furthermore, we demonstrated that ionization from specific magnetic sublevels of various hyperfine levels of Ba can be studied, and investigated the magnetic sublevel dependence in the case of the $^{138}\text{Ba}(\dots 6s 6p; ^1P_1)$ level. These types of ionization studies represent a step toward the "perfect" electron-impact ionization experiment. The target is prepared in a pure state (it is quantum-mechanically fully defined); the energy and angular distribution and the spin of the electrons are, however, still unspecified.

In naturally occurring barium, the isotopes with atomic mass units 138, 137, 136, 135, 134, 132, and 130 are present in 71.66, 11.32, 7.81, 6.59, 2.42, 0.10, and 0.10% abundance, respectively. The nuclear spin for the even isotopes is zero and for the odd isotopes is $\frac{3}{2}$. The energy-level diagram in the absence of electric or magnetic field and Zeeman splitting for ^{138}Ba in the presence of a 100-G magnetic field are shown in Fig. 1. Excitation of selected individual hyperfine levels of $\text{Ba}(\dots 6s 6p; ^1P_1)$ is feasible with a single-mode, tunable dye laser and the magnetic sublevel populations (alignment and orientation) can be controlled by the proper selection of geometry and laser polarization in the absence of magnetic field and of geometry, polarization, and frequency in the presence of magnetic field. For the ionization measurements, we applied a magnetic field of about 100 G to split the degenerate magnetic sublevels (and to collimate the electron beam). Individual magnetic sublevels of $^{138}\text{Ba}(^1P_1)$ were populated by laser pumping and subsequently ionized by electrons of well-defined energy.

The experimental arrangement for the ionization studies is shown schematically in Fig. 2. The collimated Ba beam was crossed with an energy-selected ($\Delta E_{1/2} \approx 300$ meV) electron beam at a 90° angle. The laser beam (20 mW cw, single mode) was introduced in a direction which was perpendicular to both the atomic and the electron beams, and it could be moved to cross the Ba beam upstream, at the center, or downstream of the electron-beam ionization region corresponding to "laser low," "laser center," and "laser high" geometries. (This is necessary for separating the D -level ionization from the P -level ionization.) The polarization and frequency of the laser beam were controlled and could be varied continuously. The laser beam excited a selected magnetic sublevel of a hyperfine level in

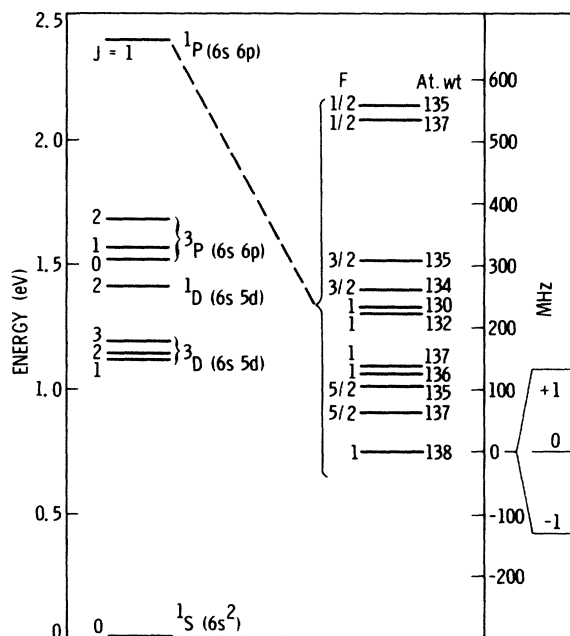


FIG. 1. Energy level diagram for Ba. On the right-hand side of the figure, the hyperfine structure is shown on an enlarged scale. The spectroscopic level designations and total angular momentum quantum numbers are indicated. Splitting of the 138 level to magnetic sublevels at 100-G field is also shown. The energy level values are from Nowicki *et al.* (Ref. 2).

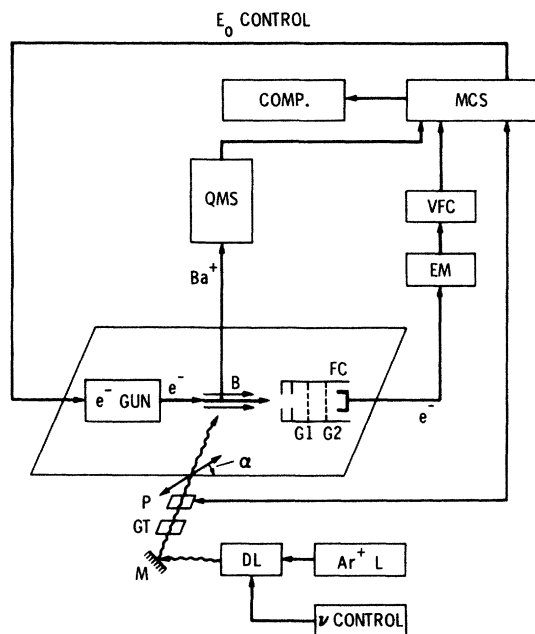


FIG. 2. Schematic diagram of the experimental arrangement. The electron, ion, and photon beams as well as the magnetic field (B) direction are shown. M , GT , and P refer to the turning mirror, Glenn-Thompson prism, and $\lambda/2$ (or $\lambda/4$) wave plate, respectively. $G1$ and $G2$ are retarding grids. FC is the Faraday cup. EM , VFC , and MCS refer to the electrometer, voltage-to-frequency converter, and multichannel scaler, respectively. The quadrupole mass spectrometer is designated as QMS . The electron impact energy and the dye-laser frequency sweep controls are indicated. For other details see text.

the 1P_1 manifold. Spontaneous emission then populated the lower lying 1D and 3D levels (we neglected cascade to the 3P level). Ions of the desired isotope were detected by a quadrupole mass spectrometer.

Figure 3 shows the $^{138}\text{Ba}^+$ signal as a function of laser frequency for three cases of laser linear polarization (α) with respect to the magnetic field (and electron beam direction). In these measurements the laser-beam and the electron-beam axes crossed the Ba beam at the same point (laser center geometry). The frequency scale is referenced to the degenerate, field-free (or $M=0$) level. The (J, M) quantum numbers for the excited state responsible for the ionization are indicated. The electron impact energy was set to 3.1 eV, which is insufficient to ionize 1S or 1D and 3D , but ionizes 1P Ba atoms. For $\alpha=0^\circ$ the selection rule $\Delta M=0$ applies (π pumping) and when the proper frequency is reached the $^1P_1(M=0)$ sublevel gets excited by the laser and in turn is ionized by the electrons. For $\alpha=90^\circ$ ($\Delta M=\pm 1$, σ^\pm pumping), the ion signal appears at the two proper frequencies. The $\alpha=45^\circ$ polarization corresponds to a linear superposition of $\alpha=0^\circ$ and $\alpha=90^\circ$ components and all three ion features are present.

The first question which arises here is whether the ionization cross sections for the magnetic sublevel species are the same. This is a situation similar to the one which arises in connection with the polarization of radiation in electron impact excitation and subsequent radiative decay

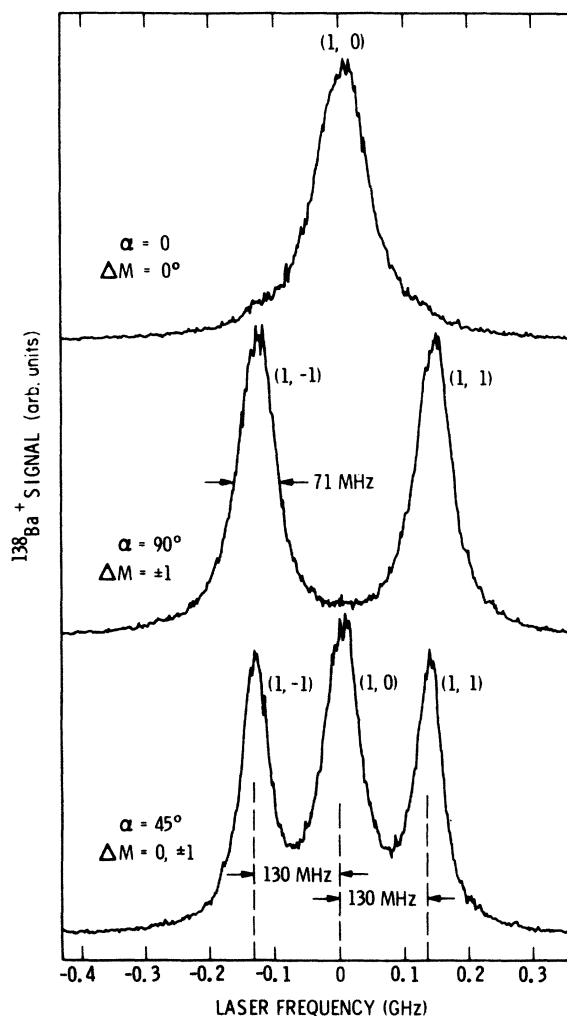


FIG. 3. $^{138}\text{Ba}^+$ signals obtained as a function of laser frequency for three linearly polarized laser pumping cases. The direction of linear polarization with respect to the magnetic field is given by α . The (J, M) values for the state responsible for the ion signal are indicated.

of atoms. In general, the observed radiation is polarized—even when no electron-photon coincidence detection is carried out and averaging over all scattered electrons applies—indicating that the magnetic sublevels are not uniformly excited by electron impact. In order to answer this question in the case of ionization (and to obtain ionization cross sections for excited species in general), the relative populations in the magnetic substates have to be determined. We addressed this question by carrying out model calculations and auxiliary measurements to guide and check the calculations. The rate equations describing the magnetic sublevel populations, which are applicable in the present case,³ were solved under steady-state conditions and the results of the calculations were experimentally verified.

In these auxiliary experiments we utilized linearly polarized ($\alpha=90^\circ$) laser light to pump the $^{138}\text{Ba}(^1P_1)$ degenerate manifold and no magnetic field was present. In the first type of experiments, we measured the $^1S \rightarrow ^1P$ dif-

ferential inelastic scattering signal with the laser on as a function of x (laser crossing point along the Ba beam) and with the laser off. The ratio of these two scattering signals yielded the ratio of the populations in the ground states (within the effective scattering volume) along the Ba beam. The decrease in the inelastic scattering intensity, with the laser on, is related to the depletion of the ground-state population in the scattering volume and corresponds to the population in excited state(s). In the second type of auxiliary experiment, we determined the $^1P \rightarrow ^1S$ superelastic scattering intensity as a function of the laser position along the Ba beam. This superelastic signal distribution (with α set to 90°) is equivalent to the distribution of relative population of $^1P(M = \pm 1)$ species in the scattering region as the laser-beam crossing is moved along the Ba-beam axis.

In comparing the results of the auxiliary experiments to the calculated population distribution, we took into account the following facts: (a) In the auxiliary experiments, no magnetic field is applied and, therefore, the degenerate $M = +1$ and $M = -1$ sublevels are coherently pumped with the linearly polarized laser beam with $\alpha = 90^\circ$. (b) The calculations deal with pure ^{138}Ba , while in the experiment the Ba beam contains all isotopes in their natural abundance ratio. (c) The calculations represent relative population distributions along the Ba beam (for a fixed position of the laser beam) as one could determine it experimentally with infinitely fine spatial resolution while in the auxiliary experiments the sampling of the population is achieved with an electron beam of finite width. Good agreement was found in the relative populations deduced from the auxiliary experiments and obtained from calculations with the corresponding experimental parameters. These studies give credence to our rate-equation modeling. Calculations show that relative population is sensitive to the $^1P_1 \rightarrow ^1S$ to $^1P_1 \rightarrow ^1D + ^3D$ branching ratio. The best agreement between calculation and experiment is obtained with a value of 300, which is consistent with the value of 280 ± 30 obtained by Lewis and co-workers⁴ very recently. Other recent investigations yielded branching ratios of 450 ± 40 ,⁵ 57 ,⁶ 550 ± 100 .⁷

The upper limit of Ba beam density, to avoid radiation trapping effects, was determined by observing the modulation of the differential $^1P \rightarrow ^1S$ superelastic signal as a function of laser linear polarization direction with respect to the scattering plane (no magnetic field is present) and lowering the Ba density until the modulation of this signal reached its maximum.

In trying to answer the question concerning the dependence of ionization cross section on magnetic sublevel for $^{138}\text{Ba}(^1P)$, we have to know the ratio of populations in the $^1P M = 0$ and $M = -1$ (or $M = +1$) sublevels and the ra-

tio of the corresponding ion signals, as well as the uncertainties in these ratios. We found under our experimental conditions that the intensity ratio was unity with $\pm 5\%$ uncertainty, and the $M = 0$ to $M = -1$ population ratio as obtained from the rate equations was $1.06 \pm 4\%$; from these we obtain that $\sigma(M = 0)/\sigma(M = -1) = 1.06 \pm 7\%$. The difference in the two cross sections is just smaller than the experimental error limit. More refined measurements are needed to come to definite conclusions.

The absolute ionization cross sections for $^{138}\text{Ba}(^1P_1, M = -1)$ and $^{138}\text{Ba}(^1D + ^3D)$, averaged over M) species were determined from threshold to 10 eV impact energy. In these measurements a magnetic field of 100 G was applied and linearly polarized laser beam pumping (with $\alpha = 90^\circ$ and proper frequency) was utilized. The cross sections were extracted from ion signal versus E_0 curves (obtained with laser off, laser low, and laser center geometries) by utilizing the calculated relative populations and the known ground-state cross sections in the following procedure.

(a) The ion signal as a function of impact energy with laser off was obtained and checked if it agreed in shape with the known ionization-cross-section curve of ground-state Ba.⁸ Normalization of the experimental ion-signal curve to the known cross-section curve then yielded the factor needed to properly scale the ion signals obtained in subsequent measurements. (It was assumed that the ground-state ionization cross section for the various isotopes was the same.) This factor includes geometrical factors and instrumental functions and applies to all laser geometries, all impact energy regions, and to all levels.

(b) The ion-signal curve obtained for the laser low arrangement was normalized and decomposed to obtain the $^{138}\text{Ba}(^1D + ^3D)$ ionization cross section $[\sigma(E_0)^D]$ curve. In region III (5.2 to 10.0 eV) both $^{138}\text{Ba}(^1D + ^3D)$ and $^{138}\text{Ba}(^1S)$ atoms contribute to the signal and we have the following relationship:

$$\frac{I(E_0)^L}{I(E_0)^{\text{off}}} \equiv R_1(E_0) = \frac{\sigma(E_0)^D N(^1D)^L + \sigma(E_0)^S N(^1S)^L}{\sigma(E_0)^S N(^1S)^{\text{off}}},$$

from which $\sigma(E_0)^D$ is obtained.

In region II the ion signal comes only from $^1D + ^3D$ ionization and the signal curve $I(E_0)^L$ can be converted to $\sigma(E_0)^D$, either by normalizing it with the factor required to normalize $I(E_0)^{\text{off}}$ to the ground-state cross section (in 1) or by arbitrarily scaling the $I(E_0)^L$ curve to match the $\sigma(E_0)^D$ curve obtained for region III. Both procedures led to the same results.

(c) The ion signal obtained with laser center geometry is decomposed and normalized to yield the $\sigma(E_0)^P$ cross sections as follows. In region III (5.2 to 10.0 eV)

$$\frac{I(E_0)^C}{I(E_0)^{\text{off}}} \equiv R_2(E_0) = \frac{\sigma(E_0)^P N(^1P)^C + \sigma(E_0)^D N(^1D)^C + \sigma(E_0)^S N(^1S)^C}{\sigma(E_0)^S N(^1S)^{\text{off}}},$$

in region II (3.8 to 5.2 eV)

$$\frac{I(E_0)^C}{I(E_0)^L} \equiv R_3(E_0) = \frac{\sigma(E_0)^P N(^1P)^C + \sigma(E_0)^D N(^1D)^C}{\sigma(E_0)^D N(^1D)^L},$$

and in region I (3.0 to 3.8 eV) the ion signal corresponds to ionization of the 1P state only and can be normalized the

same way as the ion signal corresponding to 1D ionization was normalized in region II in (b) above. Both procedures, again, lead to the same result.

The resulting ionization cross sections are shown in Fig. 4. The error limits were obtained by considering the errors associated with the populations, with the ion-signal measurements and with the ground-state cross sections used for normalization.

The ionization cross sections for the excited species are larger (by about a factor of 2 at their peak) than those for the ground state. No sharp structure larger than the experimental error limits was observed in the ionization signals. The measurements here were made for $^{138}\text{Ba}(^1P_1, M_2 = -1)$ sublevel. As indicated above we have found no substantial difference, within the experimental error limits, in ionization cross sections associated with various magnetic sublevels of the $^{138}\text{Ba}(^1P_1)$ manifold. These results are, therefore, valid for any magnetic sublevel of the 1P level (or for the average of all sublevels) within the stated error limits. No such detailed information was obtained for the $^1D + ^3D$ levels, and the cross section values in this case refer to magnetic sublevel averaged values. Very recently Bushaw, Cannon, Gerke, and Whitacker⁹ studied high-resolution laser excitation of Ba isotopes by the technique of laser-enhanced, electron-impact ionization spectroscopy. They measured the relative ionization rate of ground and 1P ^{138}Ba atoms as a function of electron impact energy with 1.3 eV electron energy resolution and found that the rate for the excited atoms was about twice as large as for the ground atoms. Further details concerning the measurements and tabulated data will be published elsewhere.¹⁰ Extension of these measurements to the higher-energy region and to other isotopes is in progress.

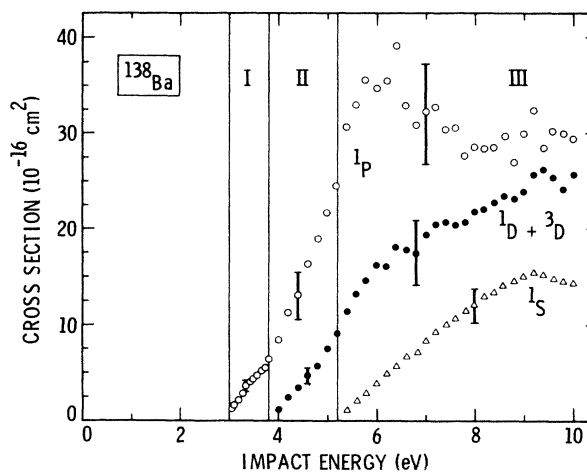


FIG. 4. Ionization cross sections for $^{138}\text{Ba } ^1S$, $^1D + ^3D$, and 1P atoms. Representative error bars are shown in each section.

We hope that these results and activities will inspire theoreticians to initiate work in this yet completely unexplored area.

Valuable discussions with R. Newell and M. R. H. Rudge, and help in setting up the experiment by W. R. Newell is gratefully acknowledged. This work was carried out at the Jet Propulsion Laboratory and was supported in part by NASA and in part by the National Science Foundation.

*Permanent address: Department of Physics, University of California, Riverside, CA 92521.

†Present address: Department of Physics, University of Kaiserslautern, Kaiserslautern, West Germany.

¹*Electron Impact Ionization*, edited by T. D. Mark and G. H. Dunn (Springer, Berlin, 1985).

²G. Nowicki, K. Bekk, S. Görling, A. Hanser, H. Rebel, and G. Schatz, *Phys. Rev. C* **18**, 2369 (1978).

³I. V. Hertel and W. Stoll, *Adv. At. Mol. Phys.* **13**, 113 (1977).

⁴D. A. Lewis, J. Kumar, M. A. Finn, and G. W. Greenlees (un-

published); M. A. Finn (private communication).

⁵G. K. Gerke and B. A. Bushaw (unpublished).

⁶E. G. Meyers, C. J. Bell, P. G. Pappas, and D. E. Murrnick, *Phys. Rev. A* **33**, 2798 (1986).

⁷S. Niggli and M. C. E. Huber (private communication).

⁸J. M. Dettmann and F. Karstensen, *J. Phys. B* **15**, 287 (1982).

⁹B. A. Bushaw, B. D. Cannon, G. K. Gerke, and T. J. Whitacker, *Opt. Lett.* **11**, 422 (1986).

¹⁰S. Trajmar and J. C. Nickel (unpublished).